

## Giant reversible magnetocaloric effect in cobalt hydroxide nanoparticles

X. H. Liu, W. Liu,<sup>a)</sup> W. J. Hu, S. Guo, X. K. Lv, W. B. Cui, X. G. Zhao, and Z. D. Zhang  
 Shenyang National Laboratory for Materials Science and International Centre for Materials Physics,  
 Institute of Metal Research, Chinese Academy of Sciences, Shenyang 110016, People's Republic of China

(Received 3 September 2008; accepted 28 October 2008; published online 17 November 2008)

The magnetocaloric effect associated with magnetic phase transitions in  $\beta$ -Co(OH)<sub>2</sub> nanoparticles has been investigated. A sign change in the magnetocaloric effect is induced by a magnetic field, which is related to a field-induced transition from the antiferromagnetic to the ferromagnetic state below the Néel temperature. The large reversible magnetic-entropy change  $-\Delta S_m$  (20.9 J/kg K at 15 K for a field change of 7 T) indicates that  $\beta$ -Co(OH)<sub>2</sub> is a potential candidate for application in magnetic refrigeration in the low-temperature range. © 2008 American Institute of Physics. [DOI: 10.1063/1.3028337]

Due to its energy-efficient and environment-friendly features, magnetic refrigeration based on the magnetocaloric effect (MCE) has recently become a promising alternative for gas-compression refrigeration technology which is presently widely used.<sup>1-10</sup> However, up to now, the MCE has been used in magnetic refrigerant devices mainly in the low-temperature range ( $T < 20$  K) by using the paramagnetic (PM) salt Gd<sub>3</sub>Ga<sub>5</sub>O<sub>12</sub>.<sup>11</sup> Therefore, it is of interest to explore magnetic refrigerant materials with a large MCE in other temperature ranges. A large MCE can be obtained near the magnetic-ordering temperature because an external magnetic field greatly influences the spin ordering. A giant MCE is usually found to be related to a field-induced first-order magnetic transition (FOMT).<sup>12-17</sup> However, a FOMT usually gives rise to considerable thermal/magnetic hysteresis which is disadvantageous for application. Therefore, much attention has been focus on finding new materials with a large MCE and a small thermal/magnetic hysteresis. A giant MCE has been observed in antiferromagnetic (AFM) systems,<sup>6,18</sup> originating from a field-induced transition from a collinear AFM to a triangular AFM [or ferromagnetic (FM)] state. As the thermal/magnetic hysteresis is quite small for the AFM systems, compared to giant-MCE FM materials, they are more suitable for application from the aspect of refrigerant efficiency and energy conservation. A few investigations have been focused mainly on the preparation and structure of cobalt hydroxide  $\beta$ -Co(OH)<sub>2</sub>.<sup>19-21</sup> The magnetic properties have been reported in Ref. 22. In this letter, we present the magnetic and magnetocaloric properties of the antiferromagnet  $\beta$ -Co(OH)<sub>2</sub> at low temperatures. A giant negative magnetic-entropy change is found, together with a field-induced MCE conversion (the MCE changes its sign in the applied magnetic field).

$\beta$ -Co(OH)<sub>2</sub> nanoparticles have been fabricated by a sol-gel method, by reacting aqueous solutions of cobalt chloride CoCl<sub>2</sub>·6H<sub>2</sub>O and sodium hydroxide NaOH at pH=12 at room temperature. The resulting gel was washed several times with distilled water until it is free from chloride ions. The gel was then dried at 353 K for 8 h to obtain  $\beta$ -Co(OH)<sub>2</sub> powder. In this process, precautions were taken to avoid any contamination to ensure the purity of the sample. The x-ray

diffraction pattern confirms the single-phase state of the particles, crystallizing in the hexagonal Mg(OH)<sub>2</sub>-type structure (space group  $P\bar{3}m1$ ).<sup>23</sup> The average grain size of the powder was determined to be about 20 nm by the Scherrer formula.<sup>24</sup> The lattice parameters  $a$  and  $c$  were determined to be 3.173 and 4.640 Å, respectively, by using the Rietveld refinement method. The magnetic properties were measured in a superconducting quantum interference device magnetometer from 4 to 300 K at applied fields up to 7 T. The powder was fixed by paraffin in a capsule in order to immobilize the randomly oriented powder particles during the measurements.

The temperature dependences of the magnetic susceptibility  $\chi$  and the inverse magnetic susceptibility in a magnetic field of 0.01 T are shown in Fig. 1. It can be seen that the  $\beta$ -Co(OH)<sub>2</sub> undergoes a PM-AFM transition at the Néel temperature of  $T_N \approx 11$  K, somewhat lower than the value of 12.3 K reported in Ref. 22. Between 200 K and the room temperature,  $\chi$  obeys the Curie-Weiss law with a positive paramagnetic Curie temperature of  $15 \pm 3$  K (20 K in Ref. 22). The effective magnetic moment per Co ion is found to be  $4.8\mu_B$  ( $5.2\mu_B$  in Ref. 22).

Figure 2 shows the magnetization curves of  $\beta$ -Co(OH)<sub>2</sub> between 4 and 28 K with  $\Delta T = 2$  K. Below  $T_N$ , the magnetization increases gradually with the applied field in the low-field range and then jumps at a critical field but remains unsaturated even at 7 T. The step in the magnetization curves

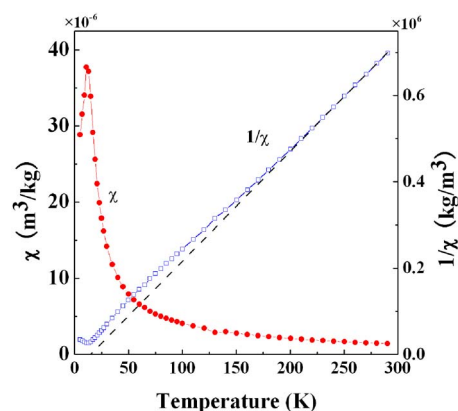


FIG. 1. (Color online) Temperature dependence of the magnetic susceptibility and the inverse magnetic susceptibility of  $\beta$ -Co(OH)<sub>2</sub> measured at an applied magnetic field of 0.01 T.

<sup>a)</sup>Author to whom correspondence should be addressed. FAX: 86-24-23891320. Electronic mail: wliu@imr.ac.cn.

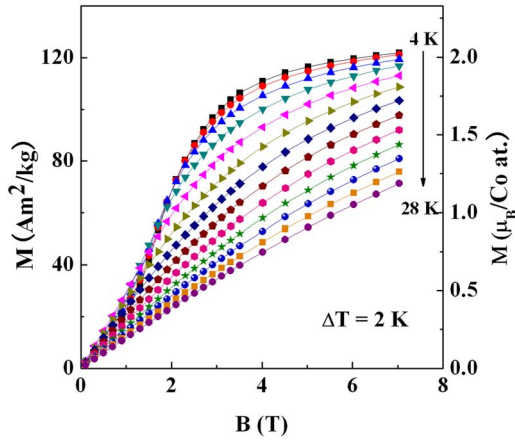


FIG. 2. (Color online) Magnetic isotherms of  $\beta$ -Co(OH)<sub>2</sub> measured between 4 and 28 K with a temperature step of 2 K.

indicates a clear field-induced AFM to FM phase transition. The critical magnetic field  $B_c$  (determined by the maximum of  $dM/dB$ ) of the magnetic transition is about 2 T. In order to further understand this magnetic transition, the temperature dependence of the magnetization  $M(T)$  in different applied fields is plotted in Fig. 3 (temperature range from 4 to 28 K with  $\Delta T=2$  K). A field-induced transition from AFM to FM state below  $T_N$  is found. The critical magnetic field (determined from the maximum of  $dM/dB$ ) for this transition is about 2 T. The inset in Fig. 3 presents  $dM/dT$  versus  $T$  curves in the applied fields of 1.7, 2.1, and 3.1 T; it is found that all the minimum values of the  $dM/dT$  are at about 15 K, indicating that the largest magnetic-entropy change may be expected at this temperature.

The magnetic hysteresis loop at 5 K in an applied field of 5 T is shown in Fig. 4. It can be noticed that the coercivity is extremely small (only about 0.008 T) and the remanent magnetization is close to zero. Furthermore, there is nearly zero magnetic hysteresis in the transition field. Compared to typical giant-MCE materials [such as Gd<sub>5</sub>(Ge<sub>1-x</sub>Si<sub>x</sub>)<sub>4</sub>,<sup>12</sup> in which the magnetic hysteresis is about 1 T near the magnetic-transition temperature], the small magnetic hysteresis of  $\beta$ -Co(OH)<sub>2</sub> is advantageous for application.

A large MCE is expected around  $T_N$  where the magnetization rapidly changes with varying temperature. The iso-

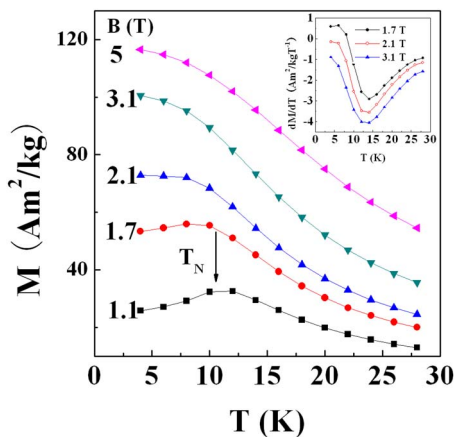


FIG. 3. (Color online) Temperature dependence of the magnetization at different magnetic fields obtained from  $M(B)$  data shown in Fig. 2. Inset:  $dM/dT$  vs  $T$  at 1.7, 2.1, and 3.1 T.

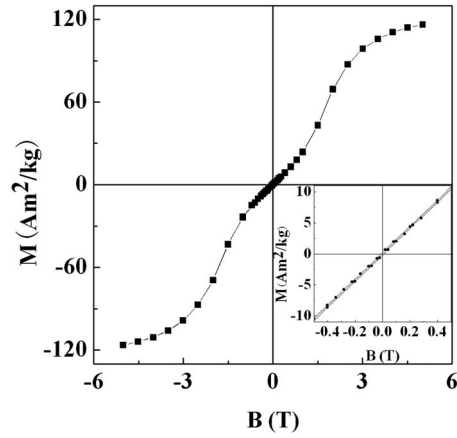


FIG. 4. Magnetic hysteresis loop of  $\beta$ -Co(OH)<sub>2</sub> at 5 K in applied fields up to 5 T. Inset: the hysteresis loop at 5 K in low fields.

thermal entropy change was derived from the magnetization data by means of the expression  $\Delta S_m(T, B) = \int_0^B (\partial M / \partial T) dB$  that can be obtained from the Maxwell relation. The curves of  $-\Delta S_m$  versus  $T$  are given in Fig. 5. It can be seen that, for small magnetic-field changes,  $-\Delta S_m$  is negative (inverse MCE) below  $T_N$ , whereas it changes to small positive values with increasing temperature. Usually, the inverse MCE is observed in first-order magnetic transitions such as AFM/FI,<sup>10</sup> AFM/FM,<sup>25</sup> or collinear AFM/triangular AFM.<sup>6</sup> The inverse MCE has also been reported in AFM/PM transition systems,<sup>7</sup> in which the applied field results in a further spin-disordered state near the transition temperature, which increases the configurational entropy.<sup>9</sup> When the applied magnetic field is higher than 3 T, a positive cusp-shaped  $-\Delta S_m$  with peak position at 15 K is observed which is consistent with the minimum value of  $dM/dT$  (inset in Fig. 3).

The inset in Fig. 5 presents  $-\Delta S_m$  versus  $\Delta B$  at 9 K, where a minimum value of  $-1.55$  J/kg K of  $-\Delta S_m$  is found for  $\Delta B=1.7$  T. The applied field destroys the antiparallel alignment of the spin moments, and the spin disorder will result in a negative  $-\Delta S_m$ , becoming more negative with increasing applied field. However, the value of  $-\Delta S_m$  increases with further increasing magnetic field due to the field-induced transition from the AFM to the FM state and becomes positive at 2.7 T. The field-induced AFM to FM tran-

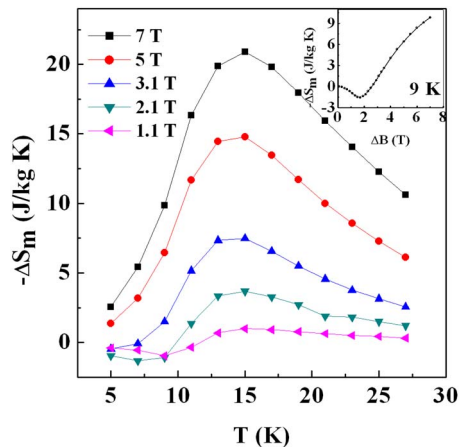


FIG. 5. (Color online) Negative magnetic-entropy change  $-\Delta S_m$  of  $\beta$ -Co(OH)<sub>2</sub> as a function of temperature for different magnetic field changes ( $\Delta B$ ). Inset:  $-\Delta S_m$  as a function of  $\Delta B$  at 9 K.

sition is responsible for the conversion from the inverse to the conventional MCE in  $\beta$ -Co(OH)<sub>2</sub>. The maximum of  $-\Delta S_m$  of 20.9 J/kg K at 15 K for  $\Delta B=7$  T is comparable with the giant MCE reported for DySb in Ref. 7 (20.6 J/kg K at 11 K for  $\Delta B=7$  T). The slope of the curve in Fig. 5 is relatively small, and the smooth variation in  $-\Delta S_m$  with temperature is more useful than a sharp one, which is another property of  $\beta$ -Co(OH)<sub>2</sub> that makes it a promising magnetorefrigerant.

In conclusion, below  $T_N$  a field-induced MCE conversion is observed in  $\beta$ -Co(OH)<sub>2</sub> due to the field-induced transition from the AFM to FM states. The giant value of  $-\Delta S_m$  (20.9 J/kg K at 15 K for the field change of 7 T) almost without hysteresis makes  $\beta$ -Co(OH)<sub>2</sub> a potential material for magnetic refrigeration in the low-temperature range.

This work has been supported by the National Nature Science Foundation of China under Project Nos. 50831006, 50331030, and 50571098.

- <sup>1</sup>C. B. Zimm, A. Jastrab, A. Sternberg, V. K. Pecharsky, K. A. Gschneidner, Jr., M. Osborne, and I. Anderson, *Adv. Cryog. Eng.* **43**, 1759 (1998).  
<sup>2</sup>J. Glanz, *Science* **279**, 2045 (1998).  
<sup>3</sup>K. A. Gschneidner, Jr., V. K. Pecharsky, and A. O. Tsokol, *Rep. Prog. Phys.* **68**, 1479 (2005).  
<sup>4</sup>E. Brück, O. Tegus, D. T. C. Thanh, and K. H. J. Buschow, *J. Magn. Mater.* **310**, 2793 (2007).  
<sup>5</sup>A. De Campos, D. L. Rocco, A. M. G. Carvalho, L. Caron, A. A. Coelho, S. Gama, L. M. da Silva, F. C. G. Gandra, A. O. dos Santos, L. P. Cardoso, P. J. von Ranke, and N. A. de Oliveira, *Nature Mater.* **5**, 802 (2006).  
<sup>6</sup>J. Du, W. B. Cui, Q. Zhang, S. Ma, D. K. Xiong, and Z. D. Zhang, *Appl.*

- Phys. Lett.* **90**, 042510 (2007).  
<sup>7</sup>W. J. Hu, J. Du, B. Li, Q. Zhang, and Z. D. Zhang, *Appl. Phys. Lett.* **92**, 192505 (2008).  
<sup>8</sup>B. Li, J. Du, W. J. Ren, W. J. Hu, Q. Zhang, D. Li, and Z. D. Zhang, *Appl. Phys. Lett.* **92**, 242504 (2008).  
<sup>9</sup>T. Krenke, E. Duman, M. Acet, E. F. Wassermann, X. Moya, L. Manosa, and A. Planes, *Nature Mater.* **4**, 450 (2005).  
<sup>10</sup>O. Tegus, E. Brück, L. Zhang, W. Dagula, K. H. J. Buschow, and F. R. de Boer, *Physica B* **319**, 174 (2002).  
<sup>11</sup>J. A. Barclay and W. A. Steyert, *Cryogenics* **22**, 73 (1982).  
<sup>12</sup>V. K. Pecharsky and K. A. Gschneidner, Jr., *Phys. Rev. Lett.* **78**, 4494 (1997).  
<sup>13</sup>O. Tegus, E. Brück, K. H. J. Buschow, and F. R. de Boer, *Nature (London)* **415**, 150 (2002).  
<sup>14</sup>H. Wada and Y. Tanabe, *Appl. Phys. Lett.* **79**, 3302 (2001).  
<sup>15</sup>F. X. Hu, B. G. Shen, J. R. Sun, Z. H. Cheng, G. H. Rao, and X. X. Zhang, *Appl. Phys. Lett.* **78**, 3675 (2001).  
<sup>16</sup>S. Gama, A. A. Coelho, A. de Campos, A. M. G. Carvalho, F. C. G. Gandra, P. J. von Ranke, and N. A. de Oliveira, *Phys. Rev. Lett.* **93**, 237202 (2004).  
<sup>17</sup>S. Stadler, M. Khan, J. Mitchell, N. Ali, A. M. Gomes, I. Dubenko, A. Y. Takeuchi, and A. P. Guimarães, *Appl. Phys. Lett.* **88**, 192511 (2006).  
<sup>18</sup>T. Samanta, I. Das, and S. Banerjee, *Appl. Phys. Lett.* **91**, 152506 (2007).  
<sup>19</sup>L. Cao, F. Xu, Y. Y. Liang, and H. L. Li, *Adv. Mater. (Weinheim, Ger.)* **16**, 1853 (2004).  
<sup>20</sup>X. L. Li, J. F. Liu, and Y. D. Li, *Mater. Chem. Phys.* **80**, 222 (2003).  
<sup>21</sup>J. T. Sampanthar and H. C. Zeng, *J. Am. Chem. Soc.* **124**, 6668 (2002).  
<sup>22</sup>T. Takada, Y. Bando, M. Kiyama, and H. Miyamoto, *J. Phys. Soc. Jpn.* **21**, 2726 (1966).  
<sup>23</sup>W. Lotmar and W. Feitknecht, *Zeitschrift fuer Kristallographie, Kristallgeometrie, Kristallphysik, Kristallchemie* **93**, 368 (1936).  
<sup>24</sup>H. P. Klug and L. E. Alexander, *X-ray Diffraction Procedures for Polycrystalline and Amorphous Materials*, 2nd ed. (Wiley, New York, 1974), Chap. 9.  
<sup>25</sup>M. P. Annaorazov, S. A. Nikitin, A. L. Tyurin, K. A. Asatryan, and A. K. Dvletov, *J. Appl. Phys.* **79**, 1689 (1996).